

Strong-coupling regime for quantum boxes in pillar microcavities: Theory

Lucio Claudio Andreani and Giovanna Panzarini

INFN, Dipartimento di Fisica "A. Volta," Università di Pavia, via Bassi 6, I-27100 Pavia, Italy

Jean-Michel Gérard

France Télécom/CNET, 196 avenue H. Ravera, F-92220 Bagneux, France

(Received 10 March 1999)

A study of quantum box transitions coupled to three-dimensionally confined photonic modes in pillar microcavities is presented, focusing on the conditions for achieving a vacuum-field Rabi splitting. For a single InAs quantum box the oscillator strength is a factor of ten too small for being in strong coupling. A calculation of exciton states localized to monolayer fluctuations in quantum wells leads to much larger values of the oscillator strengths. Single localized excitons embedded in state-of-the-art micropillars can be in strong-coupling regime with a vacuum-field Rabi splitting. [S0163-1829(99)00143-5]

One of the major trends of current semiconductor research is towards achieving a low dimensionality of electronic and photonic states. Electrons and holes are localized by a spatial variation of the band edge in quantum wells (QW's), wires, and dots; photons are instead confined by a modulation of the refractive index, e.g., in planar microcavities, photonic wires, micropillars, and microdisks.¹⁻³

A quantum box (QB) in a three-dimensional (3D) microcavity represents the "ultimate" system, where both electrons and photons are confined in all dimensions. Such a system can exhibit peculiar effects characteristic of a two-level atom in interaction with an optical cavity: strong enhancement or inhibition of the spontaneous emission rate in the weak-coupling regime, vacuum-field Rabi splitting and the formation of dressed states in the strong-coupling regime, pure quantum effects like photon squeezing and antibunching. A reduction by a factor of five of the radiative lifetime of QB transitions in pillar microcavities has been recently demonstrated.⁴ The rapid progress of epitaxial growth and nanolithography techniques, together with the development of near-field optical spectroscopy, makes the strong-coupling regime of QB's in 3D microcavities a realistic goal of research.

The present work gives a theoretical description of the crossover from weak- to strong-coupling regimes for 3D confined electronic states in pillar microcavities [or micropillars (MP's)] and provides an estimation of the vacuum-field Rabi splitting that can be attained. After a short presentation of the theory, two cases are considered for the material excitation: self-assembled InAs QB's or excitons bound to monolayer fluctuations in QW's.

We consider a single QB in a 3D microcavity. The QB is modeled by a two-level system with a transition frequency ω_0 and an isotropic dipole. The interaction Hamiltonian is $H_1 = -\mathbf{d} \cdot \mathbf{E}$, where \mathbf{d} (\mathbf{E}) is the dipole (electric-field) operator. The quantized electric field is expressed in terms of the cavity modes as⁵

$$\mathbf{E}(\mathbf{r}) = i \sum_{\mu} \left(\frac{\hbar \omega_{\mu}}{2 \epsilon_r \epsilon_0} \right)^{1/2} [\hat{a}_{\mu} \boldsymbol{\alpha}_{\mu}(\mathbf{r}) - \hat{a}_{\mu}^{\dagger} \boldsymbol{\alpha}_{\mu}^*(\mathbf{r})], \quad (1)$$

where $\hat{a}_{\mu}^{\dagger}, \hat{a}_{\mu}$ are creation and destruction operators for a cavity mode μ with frequency ω_{μ} , $\boldsymbol{\alpha}_{\mu}(\mathbf{r})$ is the normalized mode function, and ϵ_r (ϵ_0) is the relative (vacuum) permittivity (Gaussian units: $4\pi\epsilon_0 \rightarrow 1$). Each cavity mode is characterized by a quality factor Q_{μ} and a linewidth [full width at half maximum (FWHM)] $\gamma_{c,\mu} = \omega_{\mu}/Q_{\mu}$.

The spontaneous emission (SE) rate of the QB at position \mathbf{r}_1 coupled to a single-cavity mode μ is calculated in perturbation theory as

$$\gamma_{SE} = \frac{8\pi Q_{\mu}}{\hbar} \frac{|\mathbf{d} \cdot \boldsymbol{\alpha}_{\mu}(\mathbf{r}_1)|^2}{4\pi\epsilon_r\epsilon_0} \frac{(\gamma_{c,\mu}/2)^2}{(\omega_0 - \omega_{\mu})^2 + (\gamma_{c,\mu}/2)^2}. \quad (2)$$

Under resonance conditions, and if the transition dipole has the same polarization as the cavity mode,

$$\gamma_{SE} = \frac{8\pi Q_{\mu}}{\hbar} \frac{d^2}{4\pi\epsilon_r\epsilon_0} |\boldsymbol{\alpha}_{\mu}(\mathbf{r}_1)|^2 = F_{\mu} \gamma_0, \quad (3)$$

where

$$\gamma_0 = \frac{4}{3} \frac{n_r}{4\pi\epsilon_0} \frac{d^2 \omega^3}{\hbar c^3} \quad (4)$$

is the free decay rate in the medium ($n_r = \sqrt{\epsilon_r}$), and

$$F_{\mu} = \frac{3}{4\pi^2} \left(\frac{\lambda}{n_r} \right)^3 Q_{\mu} |\boldsymbol{\alpha}_{\mu}(\mathbf{r}_1)|^2 \quad (5)$$

is the enhancement/dehancement (or Purcell) factor which depends only on cavity properties.⁶ If the emitter is placed at a maximum of the electric field, as we assume in the following, the Purcell factor can also be expressed in terms of the effective mode volume \tilde{V} defined as

$$\frac{1}{\tilde{V}} = |\boldsymbol{\alpha}_{\mu}(\mathbf{r}_1)|_{\max}^2. \quad (6)$$

The coupling constant of the QB-cavity interaction is $\hbar g = |\langle \mathbf{d} \cdot \mathbf{E} \rangle|$ and can be expressed in terms of the oscillator strength (OS) $f = 2m\omega_0 d^2 / (e^2 \hbar)$ as

$$g = \left(\frac{1}{4\pi\epsilon_1\epsilon_0} \frac{\pi e^2 f}{m\tilde{V}} \right)^{1/2} \quad (7)$$

(m is the free-electron mass). This expression is similar to exciton-photon coupling for bulk exciton polaritons,⁷ f/\tilde{V} being an OS per unit volume.

The nonperturbative dynamics of the QB transition coupled to a cavity mode can be described by quantum-mechanical theory. The relevant Hamiltonian is

$$H = \hbar\omega_0\hat{\sigma}_3 + \hbar\omega_\mu(\hat{a}_\mu^\dagger\hat{a}_\mu + \frac{1}{2}) + i\hbar g(\hat{\sigma}_-\hat{a}_\mu^\dagger - \hat{\sigma}_+\hat{a}_\mu), \quad (8)$$

where $\hat{\sigma}_+$, $\hat{\sigma}_-$, $\hat{\sigma}_3$ are pseudospin operators for the two-level system with ground (excited) state $|g\rangle$ ($|e\rangle$). The spectrum of this Hamiltonian consists of a ground state $|g,0\rangle$, and of a ladder of doublets $|e,n\rangle, |g,n+1\rangle$, $n=0,1,\dots$, which in the resonance case $\omega_0 = \omega_\mu$ give rise to dressed states split by $2\hbar g\sqrt{n+1}$. However, the finite linewidths of the QB transition (γ_a) and of the cavity mode ($\gamma_{c,\mu}$) are awkward to incorporate in a Hamiltonian treatment. An appropriate procedure is to describe the linewidths as arising from coupling to reservoirs, and to work with a master equation for the density matrix $\hat{\rho}$ of the QB-cavity system:

$$\begin{aligned} \frac{d\hat{\rho}}{dt} = & \frac{1}{i\hbar}[H, \hat{\rho}] + \frac{\gamma_a}{2}[2\hat{\sigma}_-\hat{\rho}\hat{\sigma}_+ - \hat{\sigma}_+\hat{\sigma}_-\hat{\rho} - \hat{\rho}\hat{\sigma}_+\hat{\sigma}_- \\ & + \frac{\gamma_{c,\mu}}{2}[2\hat{a}_\mu\hat{\rho}\hat{a}_\mu^\dagger - \hat{a}_\mu^\dagger\hat{a}_\mu\hat{\rho} - \hat{\rho}\hat{a}_\mu^\dagger\hat{a}_\mu]. \end{aligned} \quad (9)$$

The luminescence spectrum for this model system can be calculated analytically in the limit of weak excitation, by keeping only the three lowest states $|g,0\rangle$, $|e,0\rangle$, $|g,1\rangle$.⁸ The SE spectrum for the resonant case is

$$S(\omega) \propto \left| \frac{\Omega_+ - \omega_0 + i\frac{\gamma_{c,\mu}}{2}}{\omega - \Omega_+} - \frac{\Omega_- - \omega_0 + i\frac{\gamma_{c,\mu}}{2}}{\omega - \Omega_-} \right|^2, \quad (10)$$

where⁹

$$\Omega_\pm = \omega_0 - \frac{i}{4}(\gamma_a + \gamma_{c,\mu}) \pm \sqrt{g^2 - \left(\frac{\gamma_a - \gamma_{c,\mu}}{4}\right)^2}. \quad (11)$$

Thus for $g > |\gamma_a - \gamma_{c,\mu}|/4$ the SE spectrum consists of a doublet of lines split by $2\hbar\sqrt{g^2 - (\gamma_a - \gamma_{c,\mu})^2}/16$ with the average linewidth (FWHM) $(\gamma_a + \gamma_{c,\mu})/2$; this corresponds to the formation of (slowly decaying) dressed states, or to real-time oscillations of the energy between the QB state and the field mode. The splitting between the dressed states is an intrinsic property of the coupling between the QB transition and the vacuum-field cavity mode, thus it will manifest itself as a doublet splitting in any other optical property, e.g., in reflectivity. The splitting is field-independent as long as the number n of photons in the mode is much less than 1.

The above expressions for Ω_\pm arise when solving the equations of motion for the coherences: Ω_\pm are eigenvalues for the *operator* evolution. The physics of the Jaynes-Cummings model (8) is very different from that of two

coupled harmonic oscillators, due to the fermionic nature of the QB transition. This is at variance with the case of QW excitons in planar microcavities, where the nonperturbative coupling between the exciton and the cavity mode is well described by a two-oscillator model.¹⁰ The point is that the exciton represents a collection of excited unit cells, and behaves as a boson for weak excitation, while a single QB transition is always a ‘‘fermion’’ and gives a Rabi splitting which increases as $\sqrt{n+1}$.

Let us consider the weak-coupling regime $g \ll |\gamma_{c,\mu} - \gamma_a|/4$. We assume $\gamma_{c,\mu} \gg \gamma_a$, as is usually verified for QB’s. The eigenvalues Ω_\pm then become

$$\Omega_c = \omega_0 - i\frac{\gamma_{c,\mu}}{2}, \quad (12)$$

$$\Omega_a = \omega_0 - i\left(\frac{\gamma_a}{2} + \frac{2g^2}{\gamma_{c,\mu}}\right). \quad (13)$$

The upper (lower) solution describes the cavity mode (modified QB transition). The rate of SE in the cavity mode is $\gamma_{SE} = 4g^2/\gamma_{c,\mu}$, which coincides with Eq. (3). These formulas are valid under the condition $\gamma_{SE} \ll g$, thus the perturbative regime is characterized by

$$\gamma_{SE} \ll g \ll \gamma_{c,\mu}. \quad (14)$$

In other words, the SE rate *in the cavity mode* has to be much smaller than the cavity mode width.

We now consider the situation investigated in Ref. 4, namely a QB in a cylindrical microcavity. Each MP is obtained by etching an epitaxially grown planar microcavity sample with GaAs/AlAs Bragg reflectors. The vertical Fabry-Perot cavity is a GaAs λ cavity designed to work at 0.96 μm . For pillar radii larger than about 0.5 μm , vertical confinement of the photon modes dominates over lateral dielectric confinement, which induces a shift smaller than about 0.02 eV for the lowest HE₁₁ mode. Thus we can make an ‘‘adiabatic’’ approximation and assume that vertical (z) and lateral (xy) degrees of freedom are effectively decoupled. This means that the z dependence of the electric field is given by the usual transfer-matrix approach for a planar microcavity, while the in-plane dependence is that of a cylindrical dielectric waveguide with an effective index of refraction.¹¹

With this decoupling approximation the effective volume is expressed as $\tilde{V} = \tilde{A}\tilde{L}$, where \tilde{A} is the effective area and \tilde{L} is the effective length of the vertical cavity. The latter is close to $(L_c + L_{\text{DBR}})/2$, where L_c is the cavity length and L_{DBR} is the penetration depth in the dielectric mirrors:¹⁰ since usually $L_{\text{DBR}} \approx 3L_c$, the effective length $\tilde{L} \approx 2L_c$. The effective area \tilde{A} of the lowest mode has been calculated as a function of pillar radius a . The ratio $\tilde{A}/(\pi a^2)$ is between 1/3 and 1/4, and increases with decreasing radius. Reducing the pillar radius obviously reduces the mode volume \tilde{V} , but also decreases the quality factor Q_μ due to scattering at the etched sidewalls. The ‘‘optimal’’ condition is found for a radius $a = 0.5 \mu\text{m}$, for which $Q_\mu \approx 2000$ and $\gamma_{c,\mu} \approx 0.6 \text{ meV}$ (Ref. 4): at this radius, the effective volume at a field antinode is $\tilde{V} = 0.13 (\mu\text{m})^3$.

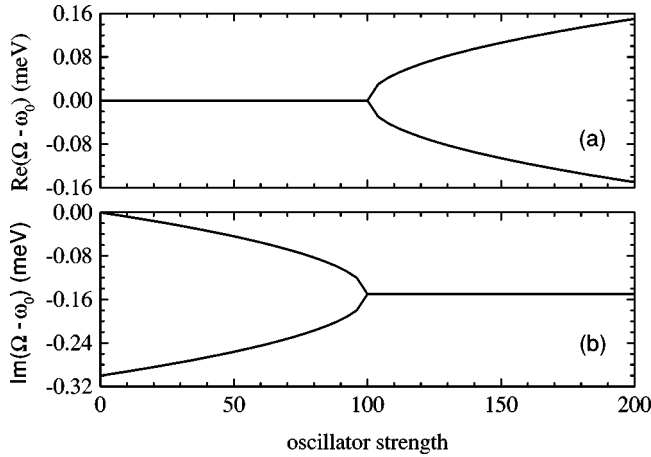


FIG. 1. (a) Real and (b) imaginary parts of the energy shift [Eq. (11)] for the coupling between the lowest HE_{11} MP mode and the QB transition, as a function of the oscillator strength, for a pillar radius $a = 0.5 \mu\text{m}$ with $Q_\mu = 2000$.

The crossover from weak to strong coupling for $a = 0.5 \mu\text{m}$ is illustrated in Fig. 1, which shows the real and imaginary parts of the energy shifts which enter the SE spectrum (10). For small OS (weak-coupling regime) the real parts coincide but the imaginary parts differ: the upper (lower) branch represents the cavity mode (modified QB transition). In this perturbative regime the lower branch in the imaginary part coincides with γ_{SE} and satisfies the inequality (14). For large OS (strong-coupling regime) a vacuum-field Rabi splitting arises. The crossover occurs for $f \sim 100$.

We now estimate the oscillator strength for the lowest transition in InAs QB's. For a small QB with infinite barrier heights, the OS tends to the value $f_0 = (4/3)(E_p/E_g)$ for bulk interband transitions. Using a Kane energy $E_p = 18 \text{ eV}$ and a transition energy $E_g = 1.3 \text{ eV}$ we get $f_0 \approx 18.5$. In real QB's this value is reduced by the anisotropic shape, leading to the removal of heavy-light hole degeneracy, and by an electron-hole overlap integral smaller than unity. Indeed, the OS measured from the integrated absorption in a sample containing InAs QB's (Ref. 12) is $f = 10.7$. This value is also in agreement with the lifetime $\tau = 1.3 \text{ ns}$ measured in Ref. 4, which [assuming a radiative origin and using Eq. (4)] leads to $f \approx 9$.

We conclude from these estimates that *a single InAs QB in state-of-the-art micropillars is in the weak-coupling regime*. For $f \sim 10$ and $a = 0.5 \mu\text{m}$ the QB-cavity coupling is $\hbar g = 0.047 \text{ meV}$, compared to $\hbar \gamma_{c,\mu}/4 \approx 0.15 \text{ meV}$; the OS should be larger by a factor of ten in order to reach the crossover to the strong-coupling regime. Although the Q factor is higher for microdisk cavities with similar mode volumes,¹³ it is still not sufficient to reach the strong-coupling regime with single InAs QB's.

In principle the vacuum-field Rabi coupling could be increased by exploiting the fact that the cavity mode interacts with all QB's, thus the effective coupling should be multiplied⁵ by a factor $\sqrt{N_{QB}}$. Since the QB's are at a maximum of the vertical profile of the field, but lie in a sheet with the same cross-sectional area of the MP, the coupling must

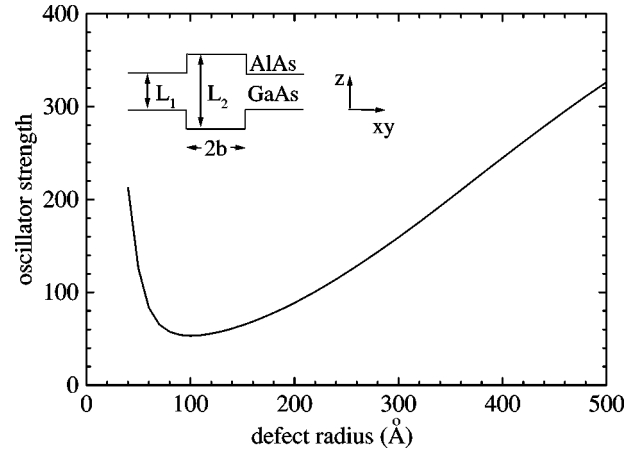


FIG. 2. Oscillator strength of the lowest heavy-hole exciton localized to a monolayer fluctuation in a GaAs/AlAs QW of width $L_1 = 40 \text{ \AA}$. Inset: model for the attractive defect.

be averaged over the transversal mode profile: as a result the effective area \tilde{A} must be replaced by the physical area A . The coupling to all QB's becomes

$$g_N = \left(\frac{2\pi}{\epsilon_r} \frac{1}{4\pi\epsilon_0} \frac{e^2 N_{QB} f}{mA(L_c + L_{DBR})} \right)^{1/2}. \quad (15)$$

This is similar to the formula for exciton-photon coupling in planar microcavities,¹⁰ with $N_{QB}f/A$ being the OS per unit area ($\sim 2 \times 10^{12} \text{ cm}^{-2}$ in the experiment of Ref. 4, leading to $g_N \sim 1 \text{ meV}$). However, the coupling should now be compared with the *total* linewidth of the QB transition, which has a very large inhomogeneous component ($\gamma_{inh} \sim 60 \text{ meV}$) due to dispersion of sizes. In practice, size dispersion prevents achieving vacuum-field Rabi splitting with a collection of QB's.

We now explore another possibility for obtaining 3D confined electronic transitions with a large OS, namely excitons bound to interface defects in narrow quantum wells. Investigations of GaAs/AlAs QW's produced with growth interruption at the interfaces have shown the formation of large interface islands, corresponding to one-monolayer (ML) fluctuations of the well thickness. Excitons become localized to these defects, as shown by local spectroscopy which displays a series of very narrow lines in photoluminescence.¹⁴ Excitons bound to ML fluctuations have a completely discretized energy spectrum and can therefore be described by the same model as for QB's.

The physics of excitons localized to interface defects can be seen by modeling the defect in a QW of width L_1 by a localized attractive potential in a disk of radius b , where the local QW thickness is $L_2 = L_1 + \text{one monolayer}$ (see the inset in Fig. 2).¹⁵ For defect radii larger than a critical value (typically $30\text{--}50 \text{ \AA}$), the lowest electron and hole subbands become localized by the lateral potential; the effective barrier height for lateral confinement is given by $E_1 - E_2$, where E_1 (E_2) is the confinement energy in the QW of width L_1 (L_2).

The behavior of the excitonic wave function can be qualitatively understood in the limiting cases of a very large or very small defect radius. For $b \gg a_B$, where a_B is the excitonic Bohr radius, the carriers are confined within the defect

and the center of mass (c.m.) of the exciton is quantized in a 2D potential well. On *increasing* the defect radius, the excitonic OS *increases* due to an increase of the area of the c.m. wave function. This behavior is similar to that of excitons in microcrystals.¹⁶ For defect radii $b \ll a_B$, instead, the carrier wave functions are laterally extended in the QW of width L_1 , and the excitonic c.m. wave function is weakly localized. On *decreasing* the defect radius, the c.m. wave function becomes less localized and the excitonic OS *increases* again with the area occupied by the c.m.. This is analog to excitons weakly bound to shallow impurities,¹⁷ and is characteristic of QW excitons bound to interface defects, since the lateral barrier height is small. Thus the OS of localized excitons must have a *minimum* at defect radii $b \sim a_B$, and must be large for very small or very large defects.

We calculate the OS of localized excitons within the above-described model of a cylindrical defect with steplike attractive potentials. The excitonic wave function is expanded in the basis of electron-hole states with different angular momenta. The resulting OS of the lowest heavy-hole exciton is shown in Fig. 2 for the case of a ML fluctuation in a GaAs/AlAs QW of width $L_1 = 40 \text{ \AA}$. The basis set is “unbiased” and no assumption about the separation of c.m. and relative variables is made, thus the calculation is expected to be valid in the whole range of radii. The behavior of the OS agrees with the expectations, with a minimum around $b \sim 100 \text{ \AA}$, and a strong increase for small or large radii. The values for large radii, where the excitonic c.m. is quantized, are of the order of the OS per unit area for the QW exciton ($\sim 8 \times 10^{12} \text{ cm}^{-2}$) multiplied by the defect area. The OS reported in Fig. 2 imply radiative lifetimes of tens to hundreds of picoseconds, as also found with related models.¹⁸ We note that even for $b = 500 \text{ \AA}$ the separation between ground and excited c.m. levels is larger than a millielectron volts, and is much larger than the lifetime broadening,

thereby allowing to resolve the excitation spectrum of *single* localized excitons.¹⁴

The results of Fig. 2 show that a localized exciton embedded in a 3D microcavity like those of Ref. 4 can be in the strong-coupling regime for both small or large defect radii. Since large defects have always a bound state, and since flat interfaces with large defects can to some extent be controlled using growth interruption, exploiting large defects is more promising. The separation between ground and excited c.m. levels should be larger than the cavity mode width, thus the useful defect radius is limited to about 500 \AA . Using ML fluctuations in GaAs/AlAs QW's requires having $\text{Al}_x\text{Ga}_{1-x}\text{As}/\text{AlAs}$ Bragg mirrors in the vertical cavity. An alternative could be the use of $\text{In}_x\text{Ga}_{1-x}\text{As}/\text{GaAs}$ QW's, or of InAs ML's in GaAs, but this is more uncertain since excitons localized at interface defects have not yet been resolved for these systems.

The conditions for achieving vacuum-field Rabi splitting for 3D confined electronic states in 3D microcavities have been derived. For a single InAs QB the oscillator strength is $f \sim 10$, which is about a factor of ten too small for being in the strong-coupling regime, with the quality factor of existing micropillars. Coupling to all QB's in the cross-sectional area results in a Rabi coupling similar to that for QW excitons, but the large inhomogeneous broadening due to size dispersion prevents from being in strong coupling. On the other hand, excitons localized to interface defects in QW's have much larger OS's, due to the large area occupied by the c.m. wave function for either small or large defects. This is shown by a detailed calculation of the excitonic states, and makes excitons bound to ML fluctuations a very promising system for achieving the strong-coupling regime for a single emitter placed in a 3D solid-state microcavity.

Useful discussions with B. Gayral are gratefully acknowledged.

¹See, e.g., *Confined Excitons and Photons: New Physics and Devices*, edited by E. Burstein and C. Weisbuch (Plenum, New York, 1995).

²See, e.g., *Microcavities and Photonic Bandgaps: Physics and Applications*, Vol. 324 of *NATO Advanced Study Institute, Series E: Applied Sciences*, edited by C. Weisbuch and J. Rarity (Kluwer, Dordrecht, 1996).

³C. Weisbuch *et al.*, Phys. Rev. Lett. **69**, 3314 (1992); J.P. Zhang *et al.*, *ibid.* **75**, 2678 (1995); J.-M. Gérard *et al.*, Appl. Phys. Lett. **69**, 449 (1996); J.P. Reithmaier *et al.*, Phys. Rev. Lett. **78**, 378 (1997); B. Ohnesorge *et al.*, Phys. Rev. B **56**, 4367 (1997).

⁴J.M. Gérard *et al.*, Phys. Rev. Lett. **81**, 1110 (1998).

⁵S. Haroche, in *Fundamental Systems in Quantum Optics*, edited by J. Dalibard, J.M. Raimond, and J. Zinn-Justin, Les Houches Session LIII (Elsevier, New York, 1992), p. 769.

⁶E.M. Purcell, Phys. Rev. **69**, 681 (1946).

⁷See, e.g., L.C. Andreani, in *Confined Excitons and Photons: New Physics and Devices* (Ref. 1), p. 57.

⁸H. Carmichael *et al.*, Phys. Rev. B **40**, 5516 (1989).

⁹Our Eq. (11) corrects a factor in the quantity λ_{\pm} in Ref. 8.

¹⁰V. Savona *et al.*, Solid State Commun. **93**, 733 (1995).

¹¹A. Yariv, *Optical Electronics* (Holt-Rinehart, New York, 1985).

¹²R.J. Warburton *et al.*, Phys. Rev. Lett. **79**, 5282 (1997).

¹³T. Baba *et al.*, IEEE Photonics Technol. Lett. **9**, 878 (1997); B. Gayral *et al.*, Appl. Phys. Lett. **75**, 1908 (1999).

¹⁴A. Zrenner *et al.*, Phys. Rev. Lett. **72**, 3382 (1994); K. Brunner *et al.*, *ibid.* **73**, 1138 (1994); D. Gammon *et al.*, *ibid.* **76**, 3005 (1996); Science **273**, 87 (1996); R. Grousson *et al.*, Phys. Rev. B **55**, 5253 (1997).

¹⁵A real defect is usually at one interface only. Here in order to have a simpler model with specular symmetry the ML fluctuation has been shared between the two interfaces.

¹⁶T. Takagahara, Phys. Rev. B **36**, 9293 (1987); E. Hanamura, *ibid.* **37**, 1273 (1988); A. Nakamura, H. Yamada, and T. Tokizaki, *ibid.* **40**, 8585 (1989).

¹⁷E.I. Rashba and G.E. Gurgenishvili, Fiz. Tverd. Tela **4**, 1029 (1962) [Sov. Phys. Solid State **4**, 759 (1962)].

¹⁸G. Bastard *et al.*, Phys. Rev. B **29**, 7042 (1984); D.S. Citrin, *ibid.* **47**, 3832 (1993); U. Bockelmann, *ibid.* **48**, 17 637 (1993).